eng

MDPI

Article

Numerical and Experimental Analyses of Flue Gas Emissions, from Biomass Pellet Combustion in a Domestic Boiler

Nevena Mileva [1,*], Penka Zlateva [1,*], Martin Ivanov [2,*], Kalin Krumov [3], Angel Terziev [2] and Adriana Comarla [4]

[1] Department of Thermal Engineering, Technical University of Varna, 9010 Varna, Bulgaria
[2] Faculty of Power Engineering and Power Machines, Technical University of Sofia, 1756 Sofia, Bulgaria; aterziev@tu-sofia.bg
[3] Faculty of Metallurgy and Material Science, University of Chemical Technology and Metallurgy, 1756 Sofia, Bulgaria; kkrumov@uctm.edu
[4] Faculty of Engineering, Constantin Brancusi University of Targu Jiu, 210185 Targu Jiu, Romania; adriana.comarla@e-ucb.ro
* Correspondence: n.mileva@tu-varna.bg (N.M.); pzlateva@tu-varna.bg (P.Z.); m_ivanov@tu-sofia.bg (M.I.)

Abstract

This study explores the combustion behavior of three biomass pellet types—wood (W), sunflower husk (SH), and a mixture of wood and sunflower husks (W/SH)—in a residential hot water boiler. Experiments were carried out under two air supply regimes (40%/60% and 60%/40% primary to secondary air) to measure flue gas concentrations of oxygen (O_2), carbon monoxide (CO), and nitrogen oxides (NO_x). The results indicate that SH pellets generate the highest emissions (CO: 1095.3 mg/m^3, NO_x: 679.3 mg/m^3), while W pellets achieve the lowest (CO: 0.3 mg/m^3, NO_x: 194.1 mg/m^3). The mixed W/SH pellets produce intermediate values (CO: 148.7 mg/m^3, NO_x: 201.8 mg/m^3). Overall boiler efficiency for all tested fuels ranged from 90.3% to 91.4%. Numerical simulations using ANSYS CFX (2024 R2 (24.2)) were performed to analyze temperature distribution, flue gas composition, and flow fields, showing good agreement with experimental outlet temperature and emission trends. These findings emphasize that both pellet composition and air distribution significantly influence efficiency and emissions, offering guidance for optimizing small-scale biomass boiler operation.

Keywords: biomass pellets; flue gas emissions; CFD modeling; combustion efficiency; residential boiler; renewable energy; emissions control

Academic Editor: Maria Founti and Fulong Zhao

Received: 3 July 2025
Revised: 11 September 2025
Accepted: 29 September 2025
Published: 2 October 2025

Citation: Mileva, N.; Zlateva, P.; Ivanov, M.; Krumov, K.; Terziev, A.; Comarla, A. Numerical and Experimental Analyses of Flue Gas Emissions, from Biomass Pellet Combustion in a Domestic Boiler. *Eng* **2025**, *6*, 257. https://doi.org/10.3390/eng6100257

1. Introduction

Sustainable energy production through renewable sources is a necessary alternative to traditional fossil fuels. Among the different forms of biofuels, pellets produced from wood and agricultural waste occupy a major place according to the authors of [1–3], due to their high energy density, combustion characteristics and the possibility of local production. Unlike solar and wind energy, whose production depends on weather conditions, biomass allows continuous and flexible energy generation, making it extremely suitable for heating in areas with a distinct seasonal temperature profile, according to the analyses in [4–6].

According to studies in [7–10], pellets are a compressed type of solid fuel with high energy density, low moisture content and stable combustion characteristics. They can be produced from different types of raw materials—pure wood, sunflower husk, straw, rice

husk, corn cob, etc. Each of these sources has its own characteristics. Although wood remains the main source of biomass in the pellet industry, according to the conclusions of the authors of [11–14], experimentation with different alternative raw materials—sunflower and rice husks, straw, nut hulls, elk sticks, etc.—is increasing. These wastes usually do not require re-cultivation or clearing and are considered as neutral in terms of greenhouse gas (GHG) emissions when used locally, as given in [15].

However, according to the analyses in [16–18], the agro-pellets often contain more alkali metals and ash, making them more challenging to combust and leading to intense slag formation, and higher emission levels. In this context, mixed pellets that combine properties of different feedstocks to achieve the required balance between calorific value, combustion stability and economic efficiency, are of increasing interest, as described in [19–21]. According to the studies in [22,23], by adding 20–40% agro-pellets to a wood base, a fuel with stable combustion, emissions according to standards and low cost can be achieved. According to the authors of [24–26], the combustion efficiency and emission level of different types of pellets depend not only on their chemical composition, but also on the air supply regime in the combustion chamber—especially on the ratio between primary and secondary air supply.

The appropriate air distribution in the boilers allows better mixing of volatile gases with oxygen, reduces carbon monoxide (CO) formation and improves the thermal stability of the combustion as described in [27,28]. For domestic boilers up to 50 kW, where the automation is simpler, this setup is particularly critical, according to [29,30]. The conclusions of the authors of [31,32] are that current trends in biomass heating include the implementation of intelligent control systems based on digital sensors, machine learning and "digital twins" of the combustion process. For the development and training of such systems, it is necessary to have validated numerical models that simulate the behavior of different pe-burn fuels under different air supply regimes, as analyzed in [33–35]. In parallel, numerical modelling methods, which are mainly computational fluid dynamics (CFD) analysis as described in [36–38], are increasingly entering the study of combustion processes in domestic pellet boilers. This, according to the authors of [39], is particularly important when different biomass mixtures are used, as flame behavior, turbulence and temperature distribution vary considerably.

The findings in [40–43] show that CFD models not only predict values of temperature, velocity and gas concentrations in real boilers, but can also save time and resources by replacing some experiments with virtual scenarios. To be reliable, these models, as described in [44,45], need to be verified and validated by real measurements of emissions, flame temperatures, and the oxygen profiles of the exhaust gases. In this way, they can be used as a method to improve combustion, such as those studied in [46,47] including in future smart systems with automatic re-adjustment of air, according to the fuel type and desired thermal load. The current research in biomass combustion offers a wealth of data on the combustion characteristics of different types of pellets, however there is insufficient information available on the interaction between fuel composition, air supply regime and emission performance, especially for mixed pellets as given in [48–50].

The authors of [51,52] focus on laboratory tests of single raw materials, while real domestic plants operate under dynamic and often unstable conditions. The use of experimentally validated CFD models creates new opportunities for the predictive and efficient design of small-scale boiler plants, based on mixed biofuels. These models, such as those made in [53–55], can be used to analyze both the internal temperature and hydrodynamic fields, and to estimate emission profiles under different air regimes and pellet types. Furthermore, according to the authors of [56,57], it is possible to simulate adaptive air-feeding

strategies—including the application of intelligent control algorithms that automatically detect the fuel and change the burner settings.

Publications on biomass combustion and the use of CFD models are increasingly being developed, as some of these studies look at the influence of pellet composition and air distribution on the emission characteristics of the domestic boilers. Limited data are also available for mixed pellets, under different air supply regimes. This study aims to present a combination of experimental measurements and a validated CFD model, allowing to evaluate the influence of fuel type and air distribution on temperature fields, emissions and combustion process efficiency.

This study proposes an approach where three different pellet types are analyzed, under two air supply regimes (60% primary/40% secondary and 40% primary/60% secondary). The analysis involves conducting experimental flue gas measurements in a real plant and building a three-dimensional CFD model in ANSYS CFX. This allows a comparison between the simulation results and the experimental data, as well as an objective assessment of the influence of the fuel composition on the emission levels and process efficiency.

2. Materials and Methods

2.1. Materials

The study was conducted by burning three types of biomass pellets, shown in Figure 1. They are as follows: type (1) is made entirely of softwood (W); type (2) consists of sunflower husk (SH), a waste product of agricultural production; type (3) is a mixture of 70% wood and 30% sunflower husk (W/SH). Their elemental composition is shown in Table 1. The selected pellets are both commonly used, such as W, and suitable alternative solutions such as SH and W/SH.

Figure 1. Studied samples: (1) wood pellets—W, (2) sunflower husk pellets—SH, (3) mixed blend pellets—W/SH.

Table 1. Characteristics of the pellets used.

Parameter	Unit	W	SH	W/SH
Carbon (C)	Wt.%	45.6	48.2	49.6
Hydrogen (H)	Wt.%	6.1	5.7	5.6
Sulfur (S)	Wt.%	0.03	0.12	0.06
Oxygen (O)	Wt.%	47.87	45.28	44.37
Nitrogen (N)	Wt.%	0.4	0.7	0.37
Ash (A)	Wt.%	0.73	2.47	0.69
Moisture (W)	Wt.%	7.47	7.42	7.07
Lower heating value (LHV)	kJ/kg	16,770	18,200	16,710

2.2. Methods

2.2.1. Experimental Setup

The experiments were conducted in a boiler, part of an operating heating plant, equipped with a pellet burner and automated fuel feeding device. The boiler was installed in a residential building and adapted to burn different types of biomasses. The main flue gas parameters were measured using a TESTO 340 portable gas analyzer (Testo, Sofia, Bulgaria), equipped with sensors for CO, NO, NO_2 and O_2 measurements. The device also allows the reading of the exhaust gas temperature. Before each series of measurements, the system shall be allowed to operate in steady state for a period of several minutes to prevent transient effects.

For each type of pellet, 15 separate measurements were carried out for each air supply mode, where the values of the concentrations of the main gas components, the flue gas temperature as well as the environmental parameters, were recorded. An uncertainty and repeatability analysis were performed to assess the accuracy and reliability of the results. The uncertainty was determined on the basis of the technical characteristics and calibration of the equipment used, and the repeatability was determined by statistical processing of 15 independent measurements for each combustion mode and pellet type. The obtained deviations are within the tolerance limits for field gas-analyzers and confirm the reliability of the presented data. The control of the air supply is ensured by manual adjustment. The overall set-up is designed to reflect the actual conditions under which domestic pellet systems operate.

2.2.2. Modelling of the Combustion Process

To study the combustion process of different types of pellets, a numerical model was developed in ANSYS CFX software environment, based on the Reynolds Averaged Navier–Stokes Equations (RANS) and the finite volume method. The same approach was used in [58], with the geometry, grid and boundary conditions retained in order to achieve a direct comparison between different types of pellets, under identical conditions.

The three-dimensional model presented in Figure 2 includes the combustion chamber, primary and secondary air inlets, fuel supply and flue gas outlet. The geometry was created, based on the actual dimensions of the boiler, part of an operating heating system of a small residential building.

The modelling uses an equivalent gas model, where the solid pellets are represented by an equivalent fuel gas mixture of methane, carbon monoxide and water vapor. This ensures adequate representation of the thermo-chemical processes and emission characteristics of the fuel.

The applied physical models and setups include a k-ε turbulent model two-stage reaction model WD2 NO PDF for methane-air, a P1 approximation for radiative heat transfer, a grid with 602,674 finite volumes and 109,329 nodes, with local compression

in the combustion and flue zones. The boundary conditions are mass flow rate and fuel mixture composition at the inlet of the combustion chamber, independent inlets for primary and secondary air, outlet conditions at atmospheric flue pressure, the heat exchanger walls are modeled as constant negative heat flux surfaces, and the remaining surfaces as adiabatic.

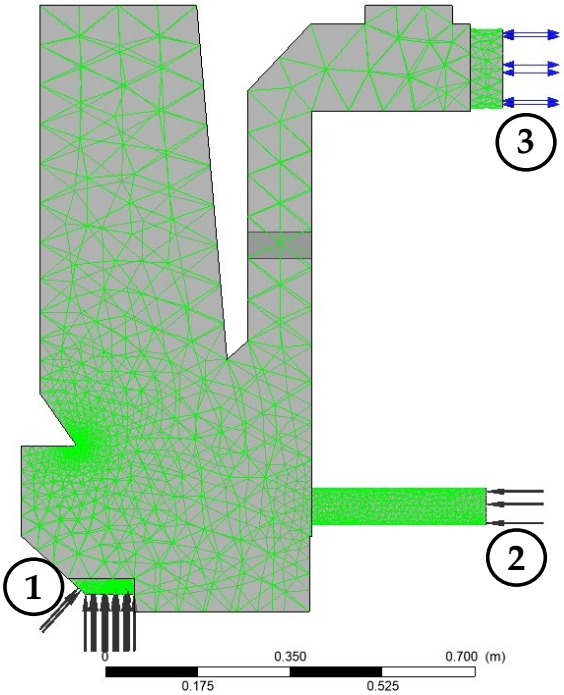

Figure 2. Three−dimensional combustion chamber model: (1) inlet, primary air, (2) inlet secondary air, (3) flue gas outlet.

Simulations were conducted under two air supply regimes, 40% primary/60% secondary air and vice versa (60%/40%), with equal heat input and equal initial conditions. Fuel parameters—calorific value, composition and flow rate—were set individually for each pellet type.

2.2.3. Numerical Simulation Approach

The objective of the numerical simulation is to evaluate different solid bi-fuel types and air supply ratios on combustion process parameters and flue gas emissions. Thus, for each type of pellets, input parameters are introduced according to their calorific value, mass flow rate, moisture content, carbon content and other basic elements. The composition of the equivalent combustion gas mixture was determined based on preliminary calculations of CH_4, CO and H_2O ratios. The aim is to achieve a realistic simulation of the volatile components of the solid fuel.

The simulations are implemented as non-steady-state problems, tracking the evolution of combustion over time until a steady quasi-steady state is reached. A time step of 0.05 s was used, with a maximum of 300 iterations at each step, and convergence was controlled by reducing the root-mean-square (RMS) deviation below 10^{-4} for all equations.

2.2.4. Model Validation Approach

The validation of the numerical model was performed by a comparative analysis, where the flue gas outlet temperature was chosen as the main parameter. This parameter is particularly suitable, as it reflects both the combustion efficiency itself and the behavior of the supply air flows and heat transfer in the boiler. The outlet temperature is the result

of the interaction between the fuel, the supply air and the design characteristics of the boiler—it therefore serves as a reliable basis for assessing the accuracy of the simulations.

For precise validation, the flue gas measurements taken during the combustion of W, SH and W/SH, were also taken at the temperatures during actual boiler operation under stable operating conditions. In parallel, from the simulations performed in ANSYS CFX under the same boundary and design conditions, the same parameter is reported (Figure 3 for W, Figure 4 for SH and Figure 5 for W/SH). The aim is to observe to what extent the numerical model can reproduce the observed temperature behavior.

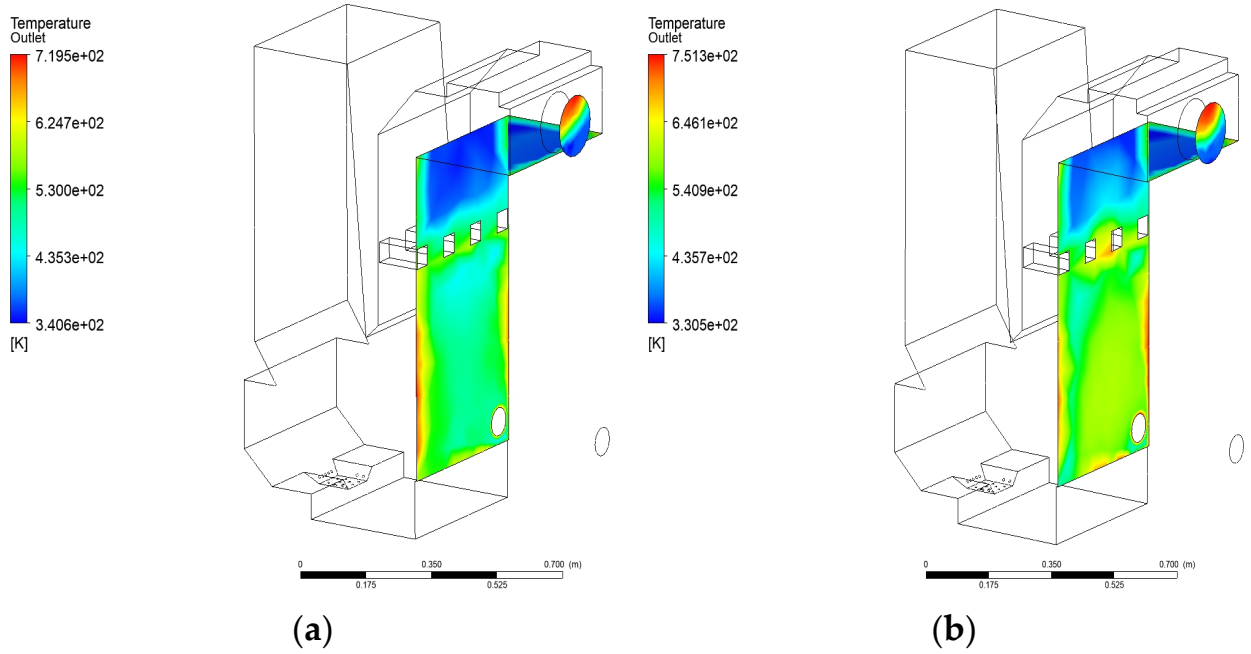

Figure 3. Temperature field distribution at the boiler outlet during combustion of W: (**a**) primary air 40%, secondary air 60%. (**b**) primary air 60%, secondary air 40%.

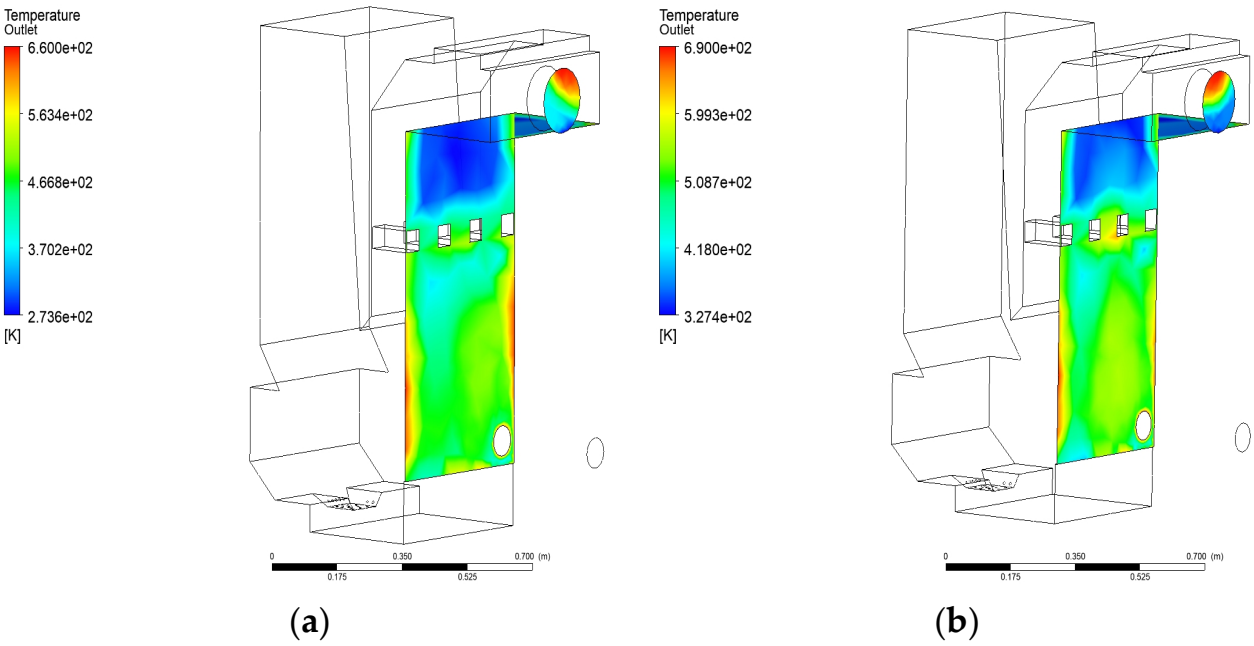

Figure 4. Temperature field distribution at the boiler outlet during combustion of SH: (**a**) primary air 40%, secondary air 60%. (**b**) primary air 60%, secondary air 40%.

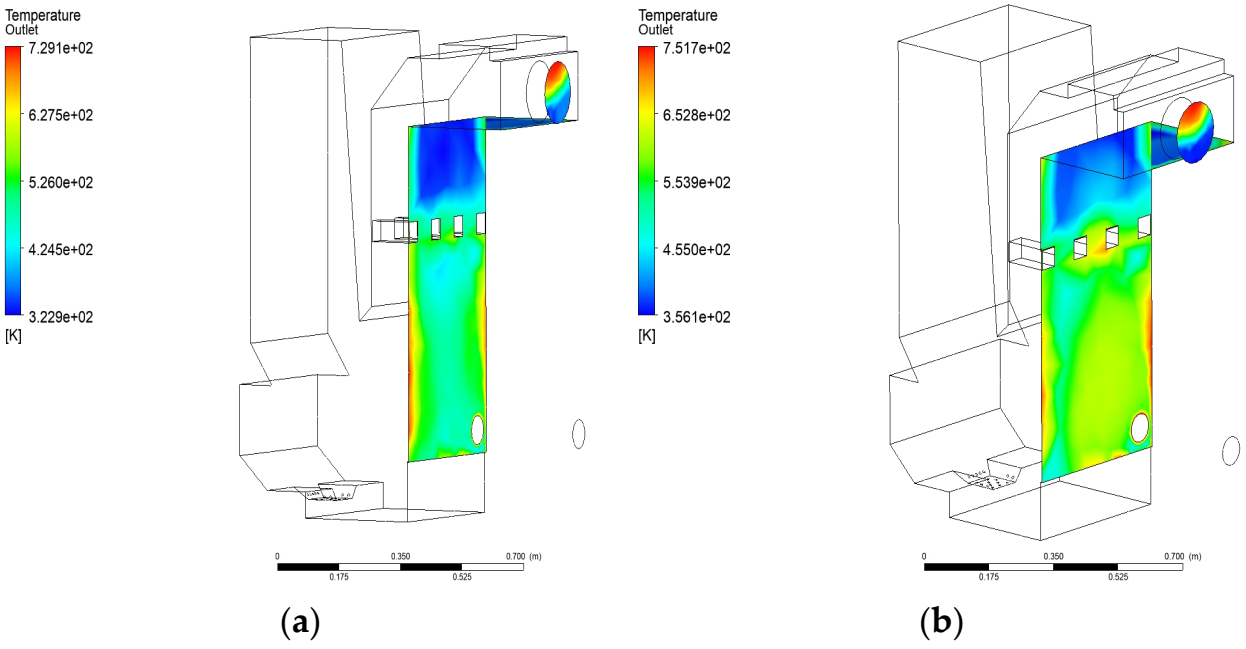

Figure 5. Temperature field distribution at the boiler outlet during combustion of W/SH. (**a**) primary air 40%, secondary air 60%. (**b**) primary air 60%, secondary air 40%.

The temperature distributions in Figure 3 for W represent some differences in the thermal structure of the burning chamber. In the 40/60 regime, a relatively uniform temperature field is observed with a distinct zone of intense combustion at the bottom of the chamber. The temperature gradient is smooth, with a gradual decrease towards the outlet, suggesting a stable combustion process and efficient mixing with the secondary air. In the 60/40 mode, a higher local temperature is observed in the upper part of the chamber and near the flue outlet, which is an indication of more intense primary combustion and partially limited mixing in the secondary zone.

In Figure 4 for SH the temperature fields show a less pronounced and lower temperature evolution, compared to the other two biofuel types. In Figure 4a, the maximum temperature remains confined to the lower zone of the combustion chamber, with the temperature field gradually expanding upwards. There is no distinct hot zone at the top, which may be due to the lower energy density of the sunflower husk and the more limited release of volatile combustible fractions. In Figure 4b, the main temperature field is localized in the middle part of the chamber, but with a higher peak temperature in the upper zone compared to Figure 4a. However, the distribution remains relatively chaotic without a distinct concentrated temperature core, which may be due to an unstable combustion process.

The temperature fields in Figure 5 represent a relatively balanced distribution in the combusting chamber. In the regime of Figure 5a, the zone of intense combustion develops mainly in the lower and middle part of the chamber. The temperature field is relatively uniform, with a smooth transition to lower values in the flue direction, indicating efficient mixing and complete combustion of the volatile components. In Figure 5b, a shift of the hot zone towards the top of the chamber and the boiler outlet is observed. This distribution is indicative of more intense primary combustion, with limited after-oxidation in the secondary zone. Although with higher local temperatures, this regime leads to a more uneven thermal load on the cladding and creates conditions for higher emissions.

The results in Figures 3–5 show the location of the main combustion and heat transfer zones in the combustion chamber. The visualizations reflect the influence of fuel type and the ratio between primary and secondary air on the flame structure and temperature

field, revealing differences in the distribution of heat fluxes and zones of intense reaction. These data are crucial for the analysis of the stability of the combustion process and for the evaluation of the emission characteristics under different operating regimes. The correlation of visual results with experimental measurements allows to establish relationships between temperature fields, combustion efficiency and pollutant emission levels, which supports the optimization of air distribution and the selection of suitable biofuels.

The selected approach allows a quick and objective comparison between real and simulated thermal response of the system. Without requiring complex interpretation of emission data, the temperature gives a direct insight into the overall combustion and thermal efficiency of the process.

3. Results

3.1. Experimental Determination of Flue Gas Parameters

In order to evaluate the behavior of the pellets during combustion, 15 independent flue gas measurements were performed for each of the three types. In order to avoid the influence of the transient state between measurements, a pre-period was provided to stabilize the combustion process, and in addition a fine-tuning of the system was performed to ensure that the exact ratio between primary and secondary air was maintained.

The average values from these measurements—including CO, NO_x, O_2 and flue gas temperature—are summarized in Table 2. The resulting data were used to develop and validate the numerical models used to simulate the combustion process.

Table 2. Averaged values of the flue gas parameters, during the combustion of the three types of pellets.

Parameter	Unit	W	SH	W/SH
O_2	Vol.%	9.15	9.5	9.34
CO_2	Vol.%	8.3	7.9	8.1
CO	mg/m^3	90.3	1095.3	148.7
NOx	mg/m^3	194.1	679.3	201.8
η	%	91.4	90.3	90.9
Temperature output	°C	72.6	75.9	74.1
Temperature Inlet	°C	52.9	55.4	53.7
Flue gas temperature	°C	96.2	98.1	96.9
Ambient temperature	°C	20.9	21.7	21.4
Engine power	kW	12.5	10.9	11.8
Air excess coefficient	λ	1.41	1.57	1.44
Fuel consumption	kg/h	7.6	7.3	6.8

3.2. Combustion Process Modelling Results

The summary results obtained by modelling the combustion process of the three types of pellets are presented in Table 3.

The results from the models for the two air supply methods show some differences in the behavior of the combustion process, depending on the pellet type. The mode with predominantly secondary air supply (40/60) leads to a more intense mixing of the fuel with the air in the combustion chamber, which improves the combustion rate for pellets with less volatile compound content. On the other hand, the 60/40 mode is more suitable for pellets with a high volatile content as it creates conditions for rapid first ignition and reaction. The assessment of the mass fractions of the components in the flue gas allows the analysis of the combustion process. The presence of methane and carbon monoxide in the fluid mixture is an indicator of incomplete reaction. In the simulation results obtained,

these components are practically absent, suggesting high combustion rates for all pellet types and air supply modes.

Table 3. Results obtained by the CFD model.

Parameter	№	W	SH	W/SH
CH_4 **	1 *	~0	~0	~0
	2 *	0	0	0
CO **	1 *	~0	~0	~0
	2 *	0	0	0
CO_2 **	1 *	25.7×10^{-2}	28.3×10^{-2}	25.4×10^{-2}
	2 *	26.9×10^{-2}	24.2×10^{-2}	25.0×10^{-2}
H_2O **	1 *	3.28×10^{-2}	2.8×10^{-2}	3.1×10^{-2}
	2 *	2.3×10^{-2}	1.9×10^{-2}	2.2×10^{-2}
N_2 **	1 *	66.5×10^{-2}	62.5×10^{-2}	66.7×10^{-2}
	2 *	64.8×10^{-2}	68.1×10^{-2}	67.3×10^{-2}
NO **	1 *	4.5×10^{-3}	6.1×10^{-3}	4.7×10^{-3}
	2 *	3.5×10^{-3}	3.4×10^{-3}	3.42×10^{-3}
O_2 **	1 *	40.1×10^{-3}	56.8×10^{-3}	41.5×10^{-3}
	2 *	56.2×10^{-3}	54.8×10^{-3}	51.6×10^{-3}
Flue gas density, kg/m^3	1 *	77.4×10^{-2}	85.1×10^{-2}	77.5×10^{-2}
	2 *	77.3×10^{-2}	80.4×10^{-2}	76.6×10^{-2}
Flue gas temperature, °C	1 *	238	199	241
	2 *	250	217	248
Flue gas velocity, m/s	1 *	73.1×10^{-2}	59.9×10^{-2}	70.3×10^{-2}
	2 *	68.4×10^{-2}	61.4×10^{-2}	69.1×10^{-2}
Flue gas mass flowrate, kg/s	1 *	-1.14×10^{-4}	-1.0×10^{-4}	-1.1×10^{-4}
	2 *	-1.15×10^{-4}	-1.0×10^{-4}	-1.11×10^{-4}

* The data in the table are for two air supply methods. (1—40/60 and 2—60/40). ** Mass share, %.

The increased CO_2 content in the exhaust is usually associated with the oxidation of organic carbon. Sunflower pellets at a 40/60 ratio exhibit the highest CO_2 values, indicating a good thermal process. Wood and mixed pellets show similar but slightly lower values, which may be the result of differences in combustion dynamics or feedstock characteristics. The H_2O concentration reflects both the moisture content of the fuel and the amount generated during combustion. The highest fraction is reported for wood pellets, which is probably due to their higher moisture content. Mixed pellets have slightly lower values, and the mixing of the raw materials leads to a better moisture balance.

N_2, presents primarily as a component of the air, and shows minimal variation between pellet types. These differences are mainly due to specific air settings and are not the result of a chemical reaction. NO levels are particularly important from an ecological point of view as it is an axis of the more harmful nitrogen compounds. The highest values are reported for sunflower pellets—probably due to the organic nitrogen content of the biomass. Mixed pellets and the 60/40 air supply had the lowest NO concentrations, confirming that air regulation is an effective way to control emissions. The O_2 concentration is more indicative of the degree of excess air. The highest values are observed for sunflower pellets, suggesting the under-utilization of the available oxygen. For wood and mixed pellets, the concentrations are lower, this is an indication of more complete and efficient combustion.

The flue gas density also varies with the type of pellet—it is highest for sunflower pellets, which is probably due to the higher CO_2 content and residual components. This may have an influence on the thermal and hydrodynamic flow characteristics and heat transfer efficiency. The temperature profile of the outlet gases is essential. The lower temperature observed for sunflower pellets (around 199 °C at 40/60) may indicate partial combustion or low energy value. In contrast, mixed pellets maintain higher temperatures (between 241 and 248 °C), suggesting better utilization of the heat potential.

The flue gas velocity affects the residence time and contact within the combustion zone. For wood pellets with a 40/60 ratio, a higher velocity (about 0.73 m/s) results in better mixing, but may shorten the response time. Mixed pellets, with a moderate velocity of about 0.69 m/s at 60/40, show the most balanced behavior. Flue gas mass flowrate is also an indicator of combustion intensity. Wood pellets and the 60/40 ratio show the highest value, which is consistent with the observed higher temperature and process dynamics. Mixed pellets show stable values and good combustion efficiency.

3.3. Model Validation

The validation of the numerical model was performed by direct comparison between the simulation and the experimentally measured flue gas temperature at the boiler outlet. This parameter was chosen as validation parameter, because it reflects the generalized efficiency of the combustion process and the heat transfer in the combustion chamber.

During the experiments, average flue gas temperature values were recorded for each pellet type. These values were compared with the results of the CFD simulations, under the same air supply conditions. The results are presented in Table 4.

Table 4. Comparison between experimental and simulated flue gas temperatures.

Pellets	Experimental Temperature, °C	Simulation Temperature, °C	Difference, °C	Deviation, %
W	96.2	98.4	+2.2	+2.29
SH	98.1	101.3	+3.2	+3.26
W/SH	96.9	95.7	−1.2	−1.24

The comparison shows good correlation between the simulated and actual measured temperatures, with differences in the ±3.5% range. This confirms that the model correctly reproduces the thermal behavior of the system and can be used with high reliability to evaluate the combustion process for different types of pellets. For the validity of the model can also be taken into account the observed consistency in the temperature dependencies between the different fuels—for sunflower pellets the highest outlet temperature is reported, while for mixed and wood pellets it is lower, but similar in value. This trend is observed equally in the simulations and the experiment, confirming the sensitivity of the model to changes in fuel composition.

Based on these results, it can be concluded that the developed numerical model has been successfully validated in terms of flue gas outlet temperature and is suitable for use in the analysis and optimization of the combustion process in domestic pellet boilers.

In addition to the flue gas outlet temperature, the experimentally measured concentrations of the main emission components—CO, NO_x and O_2—under identical operating conditions and air supply regimes, were compared for the validation of the numerical model. For this purpose, averaged values of 15 independent measurements for each mode and pellet type were used, ensuring statistical representativeness of the data. The deviations between calculated and measured values for these components are within ±10%, which is consistent with published results for boilers of the same class and power in [59]. The validation results show that the developed CFD model reproduces with a high degree of confidence both the

top-line and chemical behavior of the combustion process. This enables the model to be used as a reliable tool for investigating and optimizing the influence of different fuel types and air supply ratios on the boiler emission characteristics. This provides the necessary accuracy for the analysis of the processes that are the main focus of the present study and are directly relevant for emission reduction and fuel efficiency improvement.

Considering the validation against the averaged concentrations of the emission components (CO, NO_x and O_2), the uncertainty of the measurements was assessed by an error propagation method based on the technical characteristics of the gas analyzer sensors and repeated measurements under stable operating conditions. The combined standard uncertainty for each measured parameter was estimated to be below 5%. Additionally, a single-factor sensitivity analysis was performed where key boundary conditions (primary/secondary air ratio ±5%, pellet feed flow rate ±2%) and numerical model parameters (turbulence intensity and reaction rate constants) were varied. The results show that the predicted emission component concentrations and temperature fields remain stable within ±7% with respect to the baseline solution, confirming the robustness of the CFD model to parameter variations and the influence of measurement uncertainty, which is in agreement with the results presented in [60–62].

In order to quantify the differences between the experimental and calculated results, the Average Absolute Relative Deviation (AARD) was calculated for all investigated modes of operation, determined using the equation [63]:

$$\mathrm{AARD} = \frac{100}{N}\sum_{i=1}^{N}\left[\frac{X_{\mathrm{i,sim}} - X_{\mathrm{i,exp}}}{X_{\mathrm{i,exp}}}\right] \quad (1)$$

where $X_{\mathrm{i,sim}}$ and $X_{\mathrm{i,exp}}$ are the calculated and experimental values, respectively, and N is the number of points compared. The obtained values are in the range of 6–9%, indicating good agreement and confirming the reliability of the numerical model.

To provide a consolidated overview of the combustion characteristics of the three tested fuels, an additional graphical representation is included. Figure 6 presents a normalized diagram comprising six parameters: carbon monoxide and nitrogen oxides emissions, oxygen concentration in the flue gases, excess air ratio, combustion efficiency, and flue gas temperature. The data used in the figure are reproduced from the experimental and simulation results described earlier. This visual comparison allows simultaneous assessment of the effects of fuel composition on emission levels and thermal behavior. Wood pellets demonstrate the most favorable values, sunflower husk pellets are associated with higher emissions and temperatures, while the mixed fuel exhibits intermediate and balanced performance.

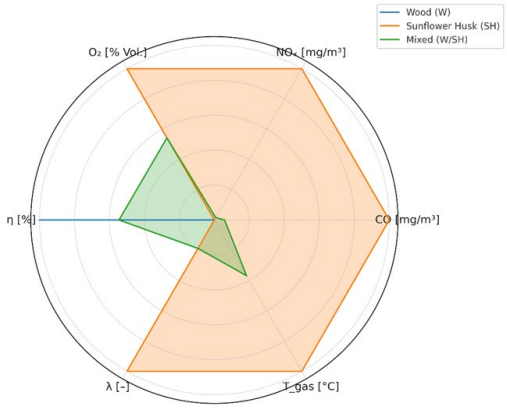

Figure 6. Normalized values of CO, NO_x, O_2, λ, η, and T (gas) for the three pellet types, showing differences in combustion behavior.

The measured emissions of carbon monoxide (CO) and nitrogen oxides (NO_x) for each pellet type are presented in Figure 7. Wood pellets result in the lowest values for both CO and NO_x, while sunflower husk pellets show the highest emissions. The mixed fuel exhibits intermediate levels, indicating a potential reduction in pollutant formation through blending.

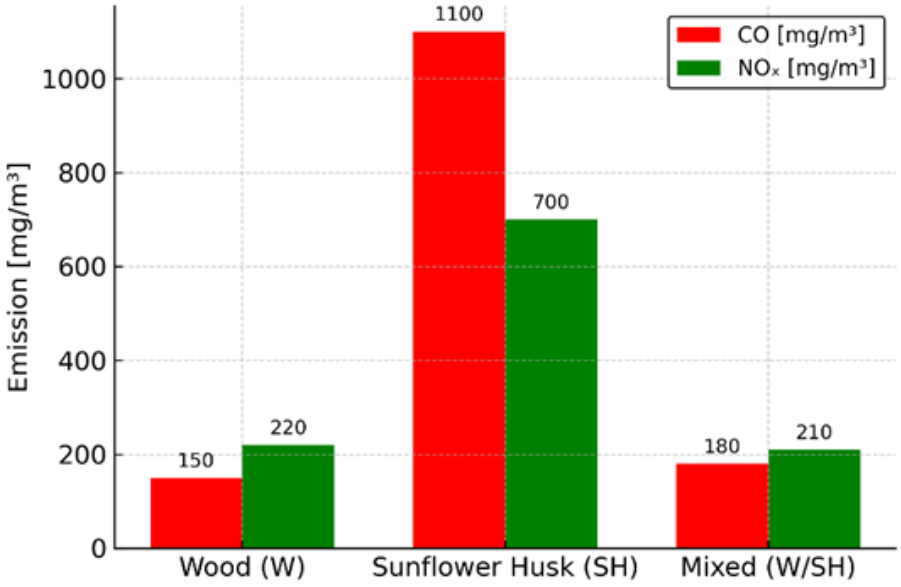

Figure 7. CO and NO_x emissions [mg/m^3] for the three pellet types.

To ensure comparability of the combustion conditions, the oxygen concentration (O_2) in the flue gases and the excess air ratio (λ) were also evaluated. As shown in Figure 8, the values remain relatively consistent across all fuel types, suggesting that differences in emission levels are primarily due to fuel composition rather than air supply variations.

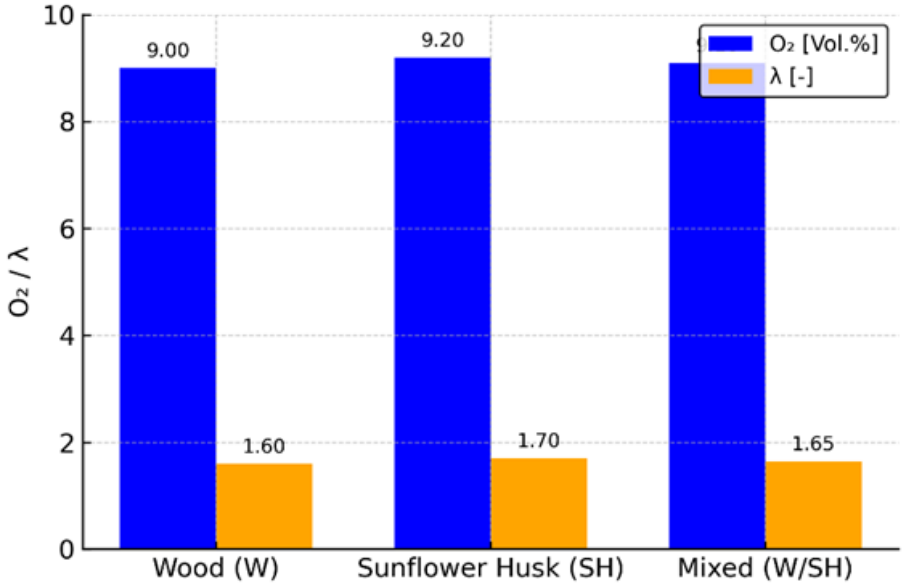

Figure 8. O_2 concentration [Vol.%] and excess air ratio (λ) during combustion.

Experimental and simulated flue gas temperatures for each pellet type are shown in Figure 9. The small deviations between both datasets confirm the accuracy of the numerical model.

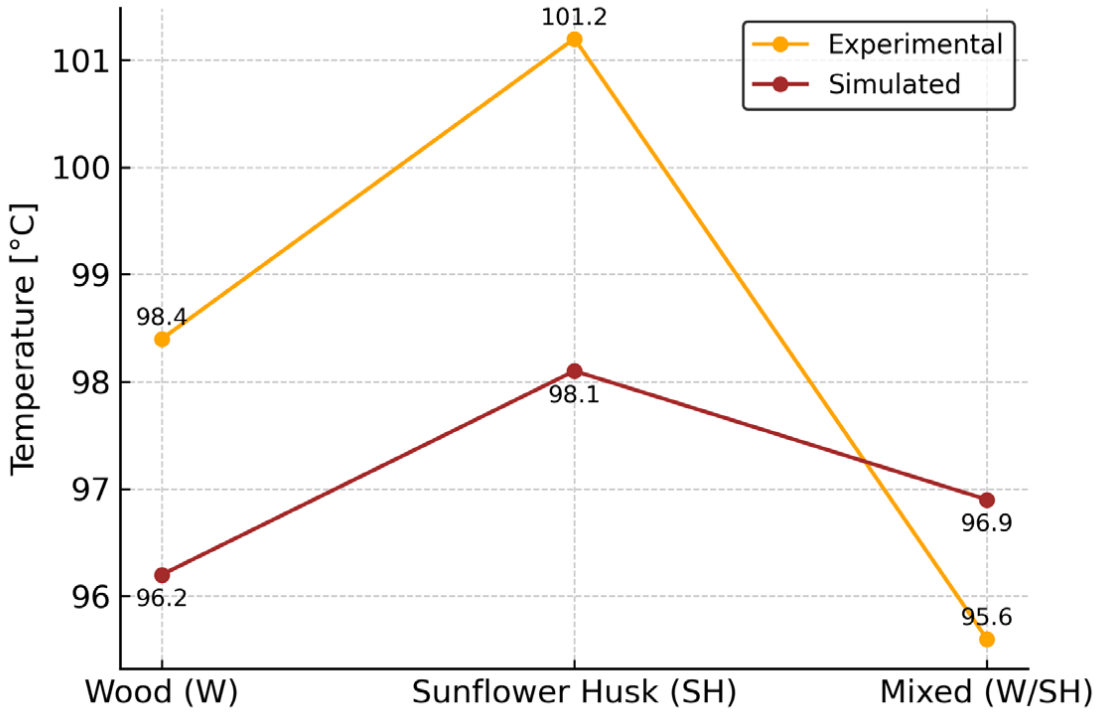

Figure 9. Comparison of simulated and experimental flue gas temperatures for the three pellet types.

In summary, the results indicate that combining different biomass fuels can offer a better balance between performance and environmental impact. The observed trends were confirmed both experimentally and through simulation, providing a solid foundation for further optimization of combustion systems.

4. Discussion

The results of the presented study show differences in the emissions profile and thermal behavior, of the three types of pellets studied. The lowest CO emissions and good combustion efficiency were observed for wood pellets, while increased CO and NO_x values were observed for agro-pellets (sunflower husks), probably related to the higher nitrogen and ash content in the biomass. Mixed pellets demonstrate intermediate behavior, with advantages both in terms of combustion stability and emission control. Similar relationships were also reported in the authors' study in [64], where agro-pellets from waste raw materials showed a tendency to slag the formation and to release higher levels of NO_x, while wood maintained cleaner combustion with lower residual gases. Studies in [65] with nut bio-pellets also noted high ash values and a specific influence on the thermal field in the combustion chamber.

In the case of the mixed pellets, the researchers in [66] indicated that combining different types of biomasses can lead to a balance between energy value and sustainable combustion, especially when a ratio of around 30% agro-biomass is maintained. This is consistent with the good performance observed for the mixed pellets in the present study. Another relevant comparison was made in [67], where instability and increased CO content were observed, when burning straw pellets in a small reactor, similar to the values reported here for pure agro-pellets. The results presented in [68] emphasize the role of air distribution in the co-combustion of wood pellets and animal waste, clearly showing a dependence between the ratio of primary and secondary air supply and the levels of the main pollutants. Adjusting this parameter leads to a reduction in CO, NO_x and fine dust emissions, accompanied by a more sustainable combustion process.

In the authors' study in [69], using both wood and agro-pellets, it was shown that CFD models can predict temperature and emission profiles with high accuracy. This is in line with the validated results in the present work, where the deviations between measured and simulated values of key parameters (CO, NO, O_2) remain within ±10%. The authors of [70] emphasize the importance of air supply and its influence on CO emissions when burning mixed biomass, especially in domestic installations. Their results support the conclusion that mixed pellets used in a 60/40 feed regime provide the most stable combustion with minimal emissions.

The results of the comparison of simulated and measured flue gas temperatures show that the numerical model used successfully represents the real processes, taking place in the combustion chamber. For all the pellets investigated, the differences are minimal, which leads to the assumption that the model is fully reliable for the assessment not only of the emissions but also of the thermal behavior of the system. The flue gas temperature at the combustion chamber outlet, as a summary indicator of combustion efficiency, complements the information obtained from the CO, NO_x and O_2 concentrations and allows a broader view of the dependence on fuel type and air supply regime, as discussed further in [70].

The measured concentrations of the main gas components confirm the influence of the fuel type and air supply modes on the emission profile of the system. The highest concentrations of CO—1095.3 mg/m^3 and NO_x—679.3 mg/m^3 were reported for the combustion of sunflower husk pellets, which is possible due to the higher nitrogen and mineral impurities content in the feedstock. Wood pellets show the lowest emissions of CO—0.3 mg/m^3 and NO_x—194.1 mg/m^3, while for mixed pellets intermediate values are reported—for CO 148.7 mg/m^3 and for NO_x 201.8 mg/m^3, confirming the potential for plant improvement by combining different biomass feedstocks. The O_2 contents of 9.15–9.5% and CO_2 of 7.9–8.3% follow the expected dependencies on the primary/secondary air ratio and indicate that a more complete oxidation of the volatile components is achieved when the amount of secondary air is increased. The results obtained are consistent with the trends better shown by the simulation model and confirm that both the chemical composition of the pellets and the air supply influence the emission profile of the boiler.

In addition to the specific measured/reported values, this study also makes an applied contribution with practical implications. A numerical model has been applied to evaluate the combustion process using different types of pellets, including those made from a mixture of wood and sunflower husk, an alternative that is increasingly the preferred raw material in heating systems. By comparing two air supply regimes and three pellet types, the relationship between pellet composition, combustion efficiency and flue gas emissions is outlined. The results presented are based on measurements under stable conditions, this provides a future reference with a practical guideline and a basis for improving the combustion regime in domestic boilers.

The application of AARD for comparison of experimental and calculated results shows that the deviations between the model and real data are within the tolerable limits (6–9%), which is in agreement with published results for analogous combustion processes in [60,63,71]. This confirms the reliability of the developed CFD model and its applicability for the analysis of combustion regimes and emission characteristics using different types of biofuels.

The measured CO and NO_x emissions show a clear dependence on the type of biomass used. Among the tested fuels, sunflower husk pellets produced the highest NO_x levels, which can be attributed to their higher nitrogen content. This trend is consistent with earlier studies reporting increased NO_x formation during the combustion of agro-residues [72,73]. In comparison, wood pellets resulted in significantly lower

emissions, as also documented in other small-scale combustion experiments [73]. The intermediate emission values recorded for the W/SH blend indicate that mixing wood and agricultural biomass can reduce the intensity of NO_x formation. Similar effects have been observed in co-combustion studies where partial substitution of straw with woody biomass lowered NO_x output by up to 40% [74]. The oxygen concentration in the flue gases remained relatively stable across all tests, with values around 9%, suggesting comparable air supply conditions. These results match previous findings on small-scale boilers operating under controlled excess air [75,76]. The similarity in O_2 levels reinforces the conclusion that the differences in CO and NO_x emissions are primarily due to fuel composition rather than differences in combustion regime. Finally, the deviation between the simulated and experimentally measured flue gas temperatures did not exceed 3 °C, which confirms that the numerical model is well calibrated. This level of agreement aligns with other validated simulation studies focused on pellet stoves and residential-scale boilers [77,78].

5. Conclusions

The conducted study shows that the type of biomass and the air supply mode affect the emission characteristics and combustion efficiency of small domestic boilers. Wood pellets provide the lowest CO emissions and stable combustion, while the agro-pellets require more precise control of flue gases, due to the higher NO and ash content. Mixed pellets, composed of wood and agro-waste, stand out with balanced combustion characteristics. They combine the advantages of the two main types of pellets and show good adaptability to different air regimes, ensuring good combustion efficiency. Numerical modeling, validated by experimental data, confirms its applicability in the assessment and optimization of processes in domestic pellet boilers. The application of CFD approaches with real input parameters provides an opportunity for predictable and sustainable design of fuel systems, tailored to the composition of the biofuels used.

The experimental results showed that sunflower husk pellets produced notably higher emissions of CO and NO_x compared to wood pellets, while the blended variant exhibited intermediate behavior. The combustion efficiency across all fuels ranged between 90.3% and 91.4%, highlighting the combined influence of fuel composition and air distribution on flue gas quality and overall combustion stability.

The CFD model applied in the study operates under steady-state conditions and does not capture the transient fluctuations inherent to real combustion processes. Consequently, the predicted gas concentrations represent averaged values and omit instantaneous variability. Despite this simplification, the model outputs are in close agreement with experimental data when comparisons are made using averaged results. The observed deviations fall within the ranges reported in similar studies on small-scale biomass boilers [66,68,70], which supports the model's suitability for assessing the effects of fuel type and air distribution, while also acknowledging its limitations in capturing dynamic combustion behavior.

Model validation using the AARD metric demonstrated agreement with experimental data within 6–9%, further supporting the credibility of the CFD approach for analyzing both combustion performance and emission characteristics.

Overall, the results emphasize the role of fuel selection in controlling emissions in small-scale biomass combustion. The validated model offers a solid foundation for future investigations focused on enhancing combustion efficiency and minimizing environmental impact through targeted design improvements in chamber geometry and air flow distribution.

Author Contributions: A.T., P.Z. and M.I.; methodology, A.T., P.Z. and N.M.; software, N.M. and K.K.; validation, K.K., N.M. and A.C.; formal analysis, A.T. and P.Z.; investigation, M.I. and K.K.; resources, N.M.; data curation, A.C. and M.I.; writing—original draft preparation, K.K., P.Z. and M.I.; writing—review and editing, P.Z. and K.K.; visualization, A.C. and N.M.; supervision, A.T.; project administration, A.T.; funding acquisition, A.T. All authors have read and agreed to the published version of the manuscript.

Funding: This study is financed by the European Union—NextGenerationEU, through the National Recovery and Resilience Plan of the Republic of Bulgaria, project No. BG-RRP-2.004-0005.

Institutional Review Board Statement: Not applicable.

Informed Consent Statement: Not applicable.

Data Availability Statement: Data are contained within the article.

Conflicts of Interest: The authors declare no conflicts of interest.

References

1. Scott, C.; Desamsetty, T.M.; Rahmanian, N. Unlocking Power: Impact of Physical and Mechanical Properties of Biomass Wood Pellets on Energy Release and Carbon Emissions in Power Sector. *Waste Biomass Valorization* **2025**, *16*, 441–458. [CrossRef]
2. Voumik, L.C.; Islam, M.A.; Ray, S.; Mohamed Yusop, N.Y.; Ridzuan, A.R. CO_2 Emissions from Renewable and Non-Renewable Electricity Generation Sources in the G7 Countries: Static and Dynamic Panel Assessment. *Energies* **2023**, *16*, 1044. [CrossRef]
3. He, B.; Yuan, X.; Qian, S.; Li, B. Carbon Neutrality: A Review. *J. Comput. Inf. Sci. Eng.* **2023**, *23*, 061101. [CrossRef]
4. Zapata, S.; Gómez, M.; Bartolomé, C.; Canalís, P.; Royo, J. Ash Behaviour during Combustion of Agropellets Produced by an Agro-Industry—Part 1: Blends Design and Experimental Tests Results. *Energies* **2022**, *15*, 1479. [CrossRef]
5. Üçok, S. Properties of Bio-Pellets Obtained from Walnut and Peanut Shells: Energy Density, Emissions and Durability. *Int. J. Agric. Biol. Eng.* **2024**, *17*, 281–285.
6. Deng, Y.; Ran, X.; Elshareef, H.; Dong, R.; Zhou, Y. Emergy, Environmental and Economic (3E) Assessment of Biomass Pellets from Agricultural Waste. *Agriculture* **2025**, *15*, 664. [CrossRef]
7. Borges, R.J.; Iturralde Carrera, L.A.; Bastida, E.J.L.; García-Martínez, J.R.; Carrillo-Serrano, R.V.; Rodríguez-Reséndiz, J. Energy Sustainability Indicators for the Use of Biomass as Fuel for the Sugar Industry. *Technologies* **2024**, *12*, 36. [CrossRef]
8. Ter-Mikaelian, M.T.; Chen, J.; Desjardins, S.M.; Colombo, S.J. Can Wood Pellets from Canada's Boreal Forest Reduce Net Greenhouse Gas Emissions from Energy Generation in the UK? *Forests* **2023**, *14*, 1090. [CrossRef]
9. Nocoń, A.; Jachimowski, A.; Koniuch, W.; Pełka, G.; Luboń, W.; Kubarek, P.; Jach-Nocoń, M.; Dawiec, D. Analysis of the Energy and Emission Performance of an Automatic Biomass Boiler in the Context of Efficient Heat Management. *Energies* **2024**, *17*, 5885. [CrossRef]
10. Echi, S.; Bouabidi, A.; Driss, Z.; Abid, M.S. CFD Simulation and Optimization of Industrial Boiler. *Energy* **2019**, *169*, 105–114. [CrossRef]
11. Gallant, R.; Farooque, A.A.; He, S.; Kang, K.; Hu, Y. A Mini-Review: Biowaste-Derived Fuel Pellet by Hydrothermal Carbonization Followed by Pelletizing. *Sustainability* **2022**, *14*, 12530. [CrossRef]
12. Zheng, Z.; Yang, W.; Yu, P.; Cai, Y.; Zhou, H.; Boon, S.K.; Subbaiah, P. Numerical Study on Combustion Characteristics of Biomass in a Cyclone Furnace under Air-Staged Conditions. *Fuel* **2020**, *259*, 116083. [CrossRef]
13. Sperandio, G.; Suardi, A.; Acampora, A.; Civitarese, V. Eco-Efficiency of Pellet Production from Dedicated Poplar Plantations. *Energies* **2024**, *17*, 3137. [CrossRef]
14. Yang, Y.; Song, L.; Li, Y.; Shen, Y.; Yang, M.; Wang, Y.; Zheng, H.; Qi, W.; Lei, T. Effects of Different Biomass Types on Pellet Qualities and Processing Energy Consumption. *Agriculture* **2025**, *15*, 316. [CrossRef]
15. Moraveji, A.; Toghraie, D. Computational Fluid Dynamics Simulation of Heat Transfer and Fluid Flow Characteristics in a Vortex Tube by Considering the Various Parameters. *Int. J. Heat Mass Transf.* **2017**, *113*, 432–443. [CrossRef]
16. Murugan, P.C.; Sekhar, S.J. Application of Computer-Based Models in Agricultural Systems: A Case Study. *Comput. Electron. Agric.* **2017**, *139*, 33–40. [CrossRef]
17. Safarian, S. Climate Impact Comparison of Biomass Combustion and Pyrolysis with Different Applications for Biochar Based on LCA. *Energies* **2023**, *16*, 5541. [CrossRef]
18. Jha, S.; Nanda, S.; Acharya, B.; Dalai, A.K. A Review of Thermochemical Conversion of Waste Biomass to Biofuels. *Energies* **2022**, *15*, 6352. [CrossRef]
19. Elsebaie, A.; Zhu, M.; Al-Abdeli, Y.M. Operational and Design Factors in Air Staging and Their Effects on Fouling from Biomass Combustion. *Sustainability* **2024**, *16*, 8584. [CrossRef]

20. Kamperidou, V. Quality Analysis of Commercially Available Wood Pellets and Correlations between Pellets Characteristics. *Energies* **2022**, *15*, 2865. [CrossRef]
21. Stolarski, M.J.; Krzyżaniak, M.; Olba-Zięty, E. Properties of Pellets from Forest and Agricultural Biomass and Their Mixtures. *Energies* **2025**, *18*, 3137. [CrossRef]
22. Yu, C.; Xiong, W.; Ma, H.; Zhou, J.; Si, F.; Jiang, X.; Fang, X. Numerical Investigation of Combustion Optimization in a Tangential Firing Boiler Considering Steam Tube Overheating. *Appl. Therm. Eng.* **2019**, *154*, 87–101. [CrossRef]
23. Rahmanta, M.A.; Aprilana, A.; Ruly; Cahyo, N.; Hapsari, T.W.D.; Supriyanto, E. Techno-Economic and Environmental Impact of Biomass Co-Firing with Carbon Capture and Storage in Indonesian Power Plants. *Sustainability* **2024**, *16*, 3423. [CrossRef]
24. Wang, Q.; Zhang, M.; Xiao, F.; Wang, H.; Jin, Y.; Hu, N.; Yang, H. Optimization of the Air Distribution in a Biomass Grate-Fired Furnace. *Energies* **2023**, *16*, 7634. [CrossRef]
25. Lavergne, S.; Larsson, S.H.; Da Silva Perez, D.; Marchand, M.; Campargue, M.; Dupont, C. Effect of Process Parameters and Biomass Composition on Flat-Die Pellet Production from Underexploited Forest and Agricultural Biomass. *Fuel* **2021**, *302*, 121076. [CrossRef]
26. Bianco, V.; Szubel, M.; Matras, B.; Filipowicz, M.; Papis, K.; Podlasek, S. CFD Analysis and Design Optimization of an Air Manifold for a Biomass Boiler. *Renew. Energy* **2021**, *163*, 2018–2028. [CrossRef]
27. Wang, Y.; Yan, L. CFD Studies on Biomass Thermochemical Conversion. *Int. J. Mol. Sci.* **2008**, *9*, 1108–1130. [CrossRef]
28. Čajová Kantová, N.; Čaja, A.; Patsch, M.; Holubčík, M.; Ďurčanský, P. Dependence of the Flue Gas Flow on the Setting of the Separation Baffle in the Flue Gas Tract. *Appl. Sci.* **2021**, *11*, 2961. [CrossRef]
29. Liu, B.; Bao, B.; Wang, Y.; Xu, H. Numerical Simulation of Flow, Combustion and NO Emission of a Fuel-Staged Industrial Gas Burner. *J. Energy Inst.* **2017**, *90*, 441–451. [CrossRef]
30. Zhang, W.; Wang, S.; Mu, L.; Jamshidnia, H.; Zhao, X. Investigation of the Forced-Convection Heat-Transfer in the Boiler Flue-Gas Heat Recovery Units Employing the Real-Time Measured Database. *Energy* **2022**, *238*, 121715. [CrossRef]
31. Tognoli, M.; Najafi, B.; Rinaldi, F. Dynamic Modelling and Optimal Sizing of Industrial Fire-Tube Boilers for Various Demand Profiles. *Appl. Therm. Eng.* **2018**, *132*, 341–351. [CrossRef]
32. Alhijazi, A.A.K.; Almasri, R.A.; Alloush, A.F. A Hybrid Renewable Energy (Solar/Wind/Biomass) and Multi-Use System Principles, Types, and Applications: A Review. *Sustainability* **2023**, *15*, 16803. [CrossRef]
33. ANSYS, Inc. *ANSYS CFX-Solver Theory Guide*; Release 2025 R1; ANSYS, Inc.: Canonsburg, PA, USA, 2025.
34. Obernberger, I.; Thek, G. Physical Characterisation and Chemical Composition of Densified Biomass Fuels with Regard to Their Combustion Behaviour. *Biomass Bioenergy* **2004**, *27*, 653–669. [CrossRef]
35. Zając, G.; Szyszlak-Bargłowicz, J.; Gołębiowski, W.; Szczepanik, M. Chemical Characteristics of Biomass Ashes. *Energies* **2018**, *11*, 2885. [CrossRef]
36. Nath, B.; Chen, G.; Bowtell, L.; Mahmood, R.A. CFDs Modeling and Simulation of Wheat Straw Pellet Combustion in a 10 kW Fixed-Bed Downdraft Reactor. *Processes* **2024**, *12*, 863. [CrossRef]
37. Wardach-Święcicka, I.; Polesek-Karczewska, S.; Kardaś, D. Biomass Combustion in the Helically Coiled Domestic Boiler Combined with the Equilibrium/Chemical Kinetics CFD Approach. *Appl. Mech.* **2023**, *4*, 779–802. [CrossRef]
38. Xu, C.; Ju, F.; Zheng, X.; Liu, Y.; Huang, J.; Li, G.; Li, Y.; Zhu, L.; Ye, L.; Pan, H. Computational Fluid Dynamics Modelling of Fixed-Bed Reactors Using Particle-Resolved Approach. *Processes* **2025**, *13*, 1820. [CrossRef]
39. Kaczyński, K.; Pełka, P. Combustion Analysis of Mixed Secondary Fuel Produced from Agro-Biomass and RDF in a Fluidized Bed. *Energies* **2024**, *17*, 2343. [CrossRef]
40. Obidziński, S.; Joka Yildiz, M.; Dąbrowski, S.; Jasiński, J.; Czekała, W. Application of Post-Flotation Dairy Sludge in the Production of Wood Pellets: Pelletization and Combustion Analysis. *Energies* **2022**, *15*, 9427. [CrossRef]
41. Gunnarsson, A.; Andersson, K.; Adams, B.R.; Fredriksson, C. Discrete-Ordinates Modelling of the Radiative Heat Transfer in a Pilot-Scale Rotary Kiln. *Energies* **2020**, *13*, 2192. [CrossRef]
42. Pafcuga, M.; Holubcik, M.; Durcansky, P.; Kapjor, A.; Malcho, M. Small Heat Source Used for Combustion of Wheat-Straw Pellets. *Appl. Sci.* **2021**, *11*, 5239. [CrossRef]
43. Royo, J.; Canalís, P.; Zapata, S.; Gómez, M.; Bartolomé, C. Ash Behaviour during Combustion of Agropellets Produced by an Agro-Industry—Part 2: Chemical Characterization of Sintering and Deposition. *Energies* **2022**, *15*, 1499. [CrossRef]
44. Álvarez-Bermúdez, C.; Chapela, S.; Varela, L.G.; Gómez, M.Á. CFD Simulation of an Internally Cooled Biomass Fixed-Bed Combustion Plant. *Resources* **2021**, *10*, 77. [CrossRef]
45. Motyl, P.; Król, D.; Poskrobko, S.; Juszczak, M. Numerical Modelling and Experimental Verification of the Low-Emission Biomass Combustion Process in a Domestic Boiler with Flue Gas Flow around the Combustion Chamber. *Energies* **2020**, *13*, 5837. [CrossRef]
46. Ion, I.V.; Popescu, F.; Mahu, R.; Rusu, E. A Numerical Model of Biomass Combustion Physical and Chemical Processes. *Energies* **2021**, *14*, 1978. [CrossRef]
47. Tańczuk, M.; Junga, R.; Werle, S.; Chabiński, M. Experimental analysis of the fixed bed gasification process of the mixtures of the chicken manure with biomass. *Renew. Energy* **2019**, *136*, 1055–1063. [CrossRef]

48. Koido, K.; Konno, D.; Sato, M. Life Cycle CO_2 Emissions and Techno-Economic Analysis of Wood Pellet Production and CHP with Different Plant Scales and Sawdust Drying Processes. *Sustainability* **2025**, *17*, 140. [CrossRef]
49. Pełka, G.; Jach-Nocoń, M.; Paprocki, M.; Jachimowski, A.; Luboń, W.; Nocoń, A.; Wygoda, M.; Wyczesany, P.; Pachytel, P.; Mirowski, T. Co mparison of Emissions and Efficiency of Two Types of Burners When Burning Wood Pellets from Different Suppliers. *Energies* **2023**, *16*, 1695. [CrossRef]
50. Lee, H.-H.; Kang, S.-B.; Choi, J.-J.; Youn, Y.-J.; Kim, K.-W.; Jeong, M.-S.; Byeon, J.-K. Co-Firing Combustion Characteristics of Woodchips and Spent Mushroom Substrates in a 400 kWth Stoker-Type Boiler. *Energies* **2022**, *15*, 9096. [CrossRef]
51. Soltero, V.M.; Chacartegui, R.; Ortiz, C.; Quirosa, G. Techno-Economic Analysis of Rural 4th Generation Biomass District Heating. *Energies* **2018**, *11*, 3287. [CrossRef]
52. Mameri, F.; Delacourt, E.; Morin, C.; Schiffler, J. 0D Dynamic Modeling and Experimental Characterization of a Biomass Boiler with Mass and Energy Balance. *Entropy* **2022**, *24*, 202. [CrossRef] [PubMed]
53. Kulkarni, A.; Mishra, G.; Palla, S.; Ramesh, P.; Surya, D.V.; Basak, T. Advances in Computational Fluid Dynamics Modeling for Biomass Pyrolysis: A Review. *Energies* **2023**, *16*, 7839. [CrossRef]
54. Silva, J.; Teixeira, S.; Teixeira, J. A Review of Biomass Thermal Analysis, Kinetics and Product Distribution for Combustion Modeling: From the Micro to Macro Perspective. *Energies* **2023**, *16*, 6705. [CrossRef]
55. Cao, H.; Jin, Y.; Song, X.; Wang, Z.; Liu, B.; Wu, Y. Computational Fluid Dynamics Simulation of Combustion and Selective Non-Catalytic Reduction in a 750 t/d Waste Incinerator. *Processes* **2023**, *11*, 2790. [CrossRef]
56. He, J.; Zhang, J.; Wang, L.; Hu, X.; Xue, J.; Zhao, Y.; Wang, X.; Dong, C. Optimizing the Controlling Parameters of a Biomass Boiler Based on Big Data. *Energies* **2023**, *16*, 7783. [CrossRef]
57. Vincenti, B.; Gallucci, F.; Paris, E.; Carnevale, M.; Palma, A.; Salerno, M.; Cava, C.; Palone, O.; Agati, G.; Caputi, M.V.M.; et al. Syngas Quality in Fluidized Bed Gasification of Biomass: Comparison between Olivine and K-Feldspar as Bed Materials. *Sustainability* **2023**, *15*, 2600. [CrossRef]
58. Zlateva, P.; Terziev, A.; Krumov, K.; Murzova, M.; Mileva, N. Research on the Combustion of Mixed Biomass Pellets in a Domestic Boiler. *Fuels* **2025**, *6*, 40. [CrossRef]
59. Bala-Litwiniak, A.; Musiał, D. Computational and Experimental Studies of Selected Types of Biomass Combustion in a Domestic Boiler. *Materials* **2022**, *15*, 4826. [CrossRef]
60. Liu, Y.; Hu, Y.; Zhou, J.; Zhu, Z.; Zhang, Z.; Li, Y.; Wang, L.; Zhang, J. Polystyrene-Supported Novel Imidazolium Ionic Liquids: Highly Efficient Catalyst for the Fixation of Carbon Dioxide under Atmospheric Pressure. *Fuel* **2021**, *305*, 121495. [CrossRef]
61. Gómez, M.Á.; Martín, R.; Collazo, J.; Porteiro, J. CFD Steady Model Applied to a Biomass Boiler Operating in Air Enrichment Conditions. *Energies* **2018**, *11*, 2513. [CrossRef]
62. Emmanouilidou, E.; Lazaridou, A.; Mitkidou, S.; Kokkinos, N.C. A Comparative Study on Biodiesel Production from Edible and Non-Edible Biomasses. *J. Mol. Struct.* **2024**, *1306*, 137870. [CrossRef]
63. Najafi, H.; Woodbury, K.A.; Beck, J.V.; Keltner, N.R. Real-Time Heat Flux Measurement Using Directional Flame Thermometer. *Appl. Therm. Eng.* **2015**, *86*, 229–237. [CrossRef]
64. Royo, J.; Canalís, P.; Quintana, D. Chemical study of fly ash deposition in combustion of pelletized residual agricultural biomass. *Fuel* **2020**, *268*, 117–228. [CrossRef]
65. Rodriguez, J.L.; Álvarez, X.; Valero, E.; Ortiz, L.; de la Torre-Rodríguez, N.; Acuña-Alonso, C. Influence of ashes in the use of forest biomass as source energy. *Fuel* **2021**, *283*, 119256. [CrossRef]
66. Royo, J.; Canalís, P.; Quintana, D.; Díaz-Ramírez, M.; Sin, A.; Rezeau, A. Experimental study on the ash behaviour in combustion of pelletized residual agricultural biomass. *Fuel* **2019**, *239*, 991–1000. [CrossRef]
67. Turzyński, T.; Kluska, J.; Ochnio, M.; Kardaś, D. Comparative Analysis of Pelletized and Unpelletized Sunflower Husks Combustion Process in a Batch-Type Reactor. *Materials* **2021**, *14*, 2484. [CrossRef]
68. Rzeźnik, W.; Rzeźnik, I.; Mielcarek-Bocheńska, P. Air Pollutants Emission during Co-Combustion of Animal Manure and Wood Pellets in a 15 kW Boiler. *Energies* **2023**, *16*, 6691. [CrossRef]
69. Horvat, I.; Dovic, D.; Filipović, P. Numerical and Experimental Methods in Development of the Novel Biomass Combustion System Concept for Wood and Agro Pellets. *Energy* **2021**, *231*, 120929. [CrossRef]
70. Mižáková, J.; Piteľ, J.; Hošovský, A.; Pavlenko, I.; Ochowiak, M.; Khovanskyi, S. Biomass Combustion Control in Small and Medium-Scale Boilers Based on Low Cost Sensing the Trend of Carbon Monoxide Emissions. *Processes* **2021**, *9*, 2030. [CrossRef]
71. Channiwala, S.A.; Parikh, P.P. A Unified Correlation for Estimating HHV of Solid, Liquid and Gaseous Fuels. *Fuel* **2002**, *81*, 1051–1063. [CrossRef]
72. Shan, Y.; Zhou, H.; Sheng, C. Ash Formation and Associated Interactions during Co-Combustion of Wheat Straw and Sewage Sludge. *Energies* **2024**, *17*, 1486. [CrossRef]
73. Tumuluru, J.S.; Lim, C.J.; Bi, X.T.; Kuang, X.; Melin, S.; Yazdanpanah, F.; Sokhansanj, S. Analysis on Storage Off-Gas Emissions from Woody, Herbaceous, and Torrefied Biomass. *Energies* **2015**, *8*, 1745–1759. [CrossRef]

74. Nyashina, G.S.; Dorokhov, V.V.; Shvedov, D.K.; Strizhak, P.A. Wood Pellets with Waste: Energy, Environmental and Mechanical Aspects. *Renew. Energy* **2025**, *250*, 123269. [CrossRef]
75. Feldmeier, S.; Schwarz, M.; Wopienka, E.; Pfeifer, C. Categorization of Small-Scale Biomass Combustion Appliances by Characteristic Numbers. *Renew. Energy* **2021**, *163*, 2128–2136. [CrossRef]
76. González, J.F.; Álvarez Murillo, A.; Díaz García, D.; Nogales-Delgado, S. The Determination of Combustion for Different Pellets Based on Ostwald Diagrams in a Domestic Stove under Experimental Conditions. *Appl. Sci.* **2023**, *13*, 12007. [CrossRef]
77. Silva, J.P.; Teixeira, S.; Teixeira, J.C. Development of a CFD Model to Study the Fundamental Phenomena Associated with Biomass Combustion in a Grate-Fired Boiler. *Processes* **2025**, *13*, 2617. [CrossRef]
78. Krawczyk, P.; Kurkus-Gruszecka, M.; Wilczyński, M.; Dzido, A. Numerical Analysis of Design and Operational Parameters of Low Power Pellet Burners. *Renew. Energy* **2025**, *243*, 122577. [CrossRef]